Side coupling of multiple optical channels by spiral patterned zinc oxide coatings on large core plastic optical fibers

Hazli Rafis Bin Abdul Rahim[1,2,3], Somarapalli Manjunath[4], Hoorieh Fallah[2], Siddharth Thokchom[5], Sulaiman Wadi Harun[1,2], Waleed Soliman Mohammed[6], Louis Gabor Hornyak[7], Joydeep Dutta[8]

[1]*Department of Electrical Engineering, Faculty of Engineering, University of Malaya, 50603 Kuala Lumpur, Malaysia*
[2]*Photonics Research Centre, University of Malaya, 50603 Kuala Lumpur, Malaysia*
[3]*Faculty of Electronic and Computer Engineering, Universiti Teknikal Malaysia Melaka, 76100 Melaka, Malaysia*
[4]*School of Electronic Engineering, Vellore Institute of Technology University, 632014 Vellore, India*
[5]*School of Technology, Assam Don Bosco University, Airport Road, Azara, Guwahati 781017, Assam, India.*
[6]*Center of Research in Optoelectronics, Communication and Control Systems (BU-CROCCS), School of Engineering, Bangkok University, 12120 Patumthani, Thailand*
[7]*Center of Excellence in Nanotechnology, Asian Institute of Technology, 12120 Patumthani, Thailand*
[8]*Chair of Functional Materials division, KTH Royal Institute of Technology, Stockholm, Sweden*
E-mail: waleed.m@bu.ac.th

Published in Micro & Nano Letters; Received on 27th October 2015; Revised on 7th December 2015; Accepted on 4th January 2016

Improved optical side coupling efficiency was demonstrated for spiral patterned zinc oxide (ZnO) nanorods coated large core plastic optic fibers (POFs) as opposed to unpatterned continuous coatings. ZnO nanorods were grown by the hydrothermal method directly onto POF surfaces. Nanorods coating enhanced coupling inside the fiber by scattering light but were also capable of causing leakage. Structuring the growth to specific regions allows scattering from different segments along the fiber to contribute to the total coupled power. ZnO nanorods growth time of 12 h and temperature of 90 °C provided the best coupling voltage. Side coupling was measured to be a factor of 2.2 times better for spiral patterned coatings as opposed to unpatterned coatings. The formation of multiple segments was as well used for multiple-wavelength channels excitation where different bands were side coupled from different segments.

1. Introduction: Zinc oxide (ZnO) is a versatile wide-bandgap (3.37 eV) semiconductor material that has contributed to the development of numerous applications over the past few years. Depending on its doping condition, ZnO can be conductive (including n-type and p-type conductivity), semi-conductive, insulating, transparent and show piezoelectric behaviour, room temperature ferromagnetism, and huge magneto-optic and chemical sensing properties [1]. This versatility makes ZnO a suitable material for a variety of integrated nanosystems that include optoelectronics [2–5], biosensors [6–8], resonators [9], medical devices [10, 11], imaging [12, 13], and wireless communication [14]. In optical fiber systems, light is typically introduced from one end, guided through the fiber and collected at the other end. This common method has been widely used for sensing applications using plastic optic fiber (POF) coated with ZnO nanostructures [15–17]. In previous work, we have demonstrated the feasibility of side coupling to optical fibers by exploiting the scattering properties of ZnO nanorods coated on silica multimode optical fibers [18]. Light induced by scattering at angles larger than the critical angle is guided inside the fiber.

Although ZnO nanorods enhance optical guidance in this way, they are also responsible for light leakage due to the very same scattering property. In our previous work, coupling of light to the core mode was accomplished by exposing the core to wet chemical etching. Light was then allowed to couple from an intermediate region near the beginning of the core exposure domain while leakage was minimised at unetched fiber domains downstream. The primary limitation of this method was that only a small portion of the fiber could be used for signal collection. This situation is undesirable for applications such as receivers in telecommunications and sensing where extended light sources are required. The extended light source leads to less guidance of light inside the fiber resulting in low efficiency and sensitivity.

To increase the magnitude of light collection, we proposed two approaches that were executed simultaneously. First, a large-core plastic fiber optic is required to increase the scattering area; and second, a structured scattering layer tightly bound to the surface of the POF is required to harvest light from different segments of the POF. The scattering layer consists of ZnO nanorods as a fiber coating. Fig. 1 illustrates the mechanism of light scattering for unpatterned (Fig. 1*a*) and spiral patterned (Fig. 1*b*) ZnO nanorods layers and for the multi-channel optical fiber case (Fig. 1*c*). Light scattering is induced by the presence of ZnO nanorods on the surface excitation locations along the POF. A portion of the scattered light is guided when scattering angles are greater than the critical angle between the surrounding and the core [19]. The coupled light propagates through the POF to the terminal detector (I_{out}). The presense of the nanorods as well causes light leakage through the side of the fiber (I_{leak}) (Fig. 1*a*). For example, if two point light sources, $P(z_1)$ and $P(z_2)$ along a POF are illuminated simultaneously, then the excitation inside the fiber is maximised at these points. However, due to the nanorods induced leakage, the intensity of the guided light decreases exponentially to the ZnO nanorods interface. For the location farthest away from the interface (e.g. z_2), any light reaching the detector is minimised. Hence, the power coupled from point z_2 provides only minimal contribution to the total guidance. Clearly, the way to increase the contribution originating from point z_2 is to reduce the amount of leakage.

Light leakage can be minimised by reducing the ZnO coverage through the application of a spiral patterned layer of ZnO nanorods as shown in Fig. 1*b*. The reduction of the effective area of the scattering layer is expected to increase the contribution from point z_2. Considering an arbitrary point at the middle of the spiral patterned ZnO layer (Fig. 1*b*), the light coupled inside the fiber leaks exponentially inside the coated region. The intensity remains steady in the uncoated region till the next ZnO patterned region where the

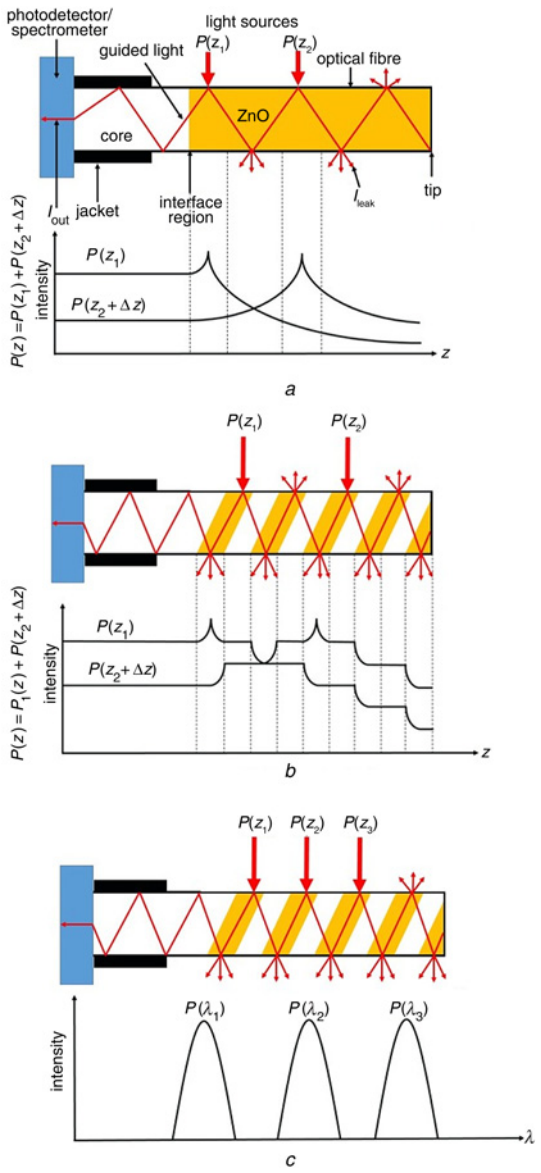

Fig. 1 *Schematic diagram of light scattering for*
a Unpatterned growth of ZnO nanorods with the coupling light
b Spiral patterned growth of ZnO nanorods with more interface and ZnO regions with the coupling light
c Spiral patterned growth of ZnO nanorods for a multi-channel excitation

exponential decay occurs again. The intensity from point z_2 is increased due to a balance between the optimised side coupling from the ZnO patches and the reduction of the leakage due to the reduction of the effective ZnO nanorods region. On the basis of this hypothesis, one can predict possible enhancement of the total coupling when an extended light source is used.

In another demonstration, the presence of patches of ZnO nanorods was used for multi-channel excitation. Though, it is possible to achieve multi-wavelength excitation with unpatterned growth, channels further from the ZnO edge suffers a sever loss. Higher power is then required for channel equalisation. This effect is minimised here using the spiral patterned POF as shown in Fig. 1*c*. Different wavelengths of light source, $P(z_1)$, $P(z_2)$, and $P(z_3)$ are individually excited at different spiral patches of ZnO nanorods. Due to the reduction of the effective scattering area, the peaks of the coupled light are expected to be higher than multi-channel performed on unpatterned ZnO nanorods growth. This gives rise to a possible application in wavelength division multiplexing. The coupling efficiency of each channel depends on the spacing between the scattering domains.

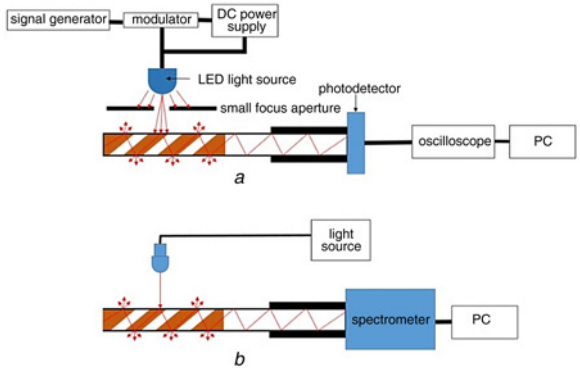

Fig. 2 *Optical characterisation apparatus*
a V_{pp} characterisation setup to measure the scattering effect of ZnO nanorods for unpatterned and spiral patterned ZnO nanorods
b Spectral analysis setup to determine wavelength coupling maxima

2. Materials, fabrication, and characterisation

2.1. Fibre preparation: Standard multimode SK-80 POF fibers (Mitsubishi Rayon Co., LTD; Japan) were used in experiments. The fiber core consists of polymethyl methacrylate resin with diameter ranging from 1840 to 2080 µm. The core is surrounded by a fluorinated polymer jacket with inner–outer diameter in the range of 1880–2120 µm, respectively. Fig. 3*a* depicts a graphical representation of the spiral structure. At first, the jacket of the POF is mechanically stripped to expose the core fiber over a length of 7 cm. Following cleansing with a dry tissue, the spiral template is applied with plastic tape (Fig. 3*a*). This work focuses on creating spiral pattern using the plastic tape (0.4 cm). The width of spiral ZnO patterned on POF was 0.2 cm. The tape was removed before experimental characterisation to expose the bare templated POF surface.

2.2. ZnO seeding procedure: The synthesis of ZnO nanorods was accomplished as previously reported [20]. First, ZnO seed particles were synthesised by dissolving ca. 0.0044 g zinc acetate dihydrate [$Zn(O_2CCH_3)_2{\cdot}2H_2O$] (Merck KGaA, Germany) in 20 ml of ethanol (Merck KGaA, Germany) to form a 1 mM solution. The resulting ZnO seed particles served as nucleation centres for nanorods growth. Unpatterned and spiral patterned POFs were then dipped into the ZnO seed solution for 30 s and placed on a hotplate set at 70 °C for 2 min. The solvent was then allowed to

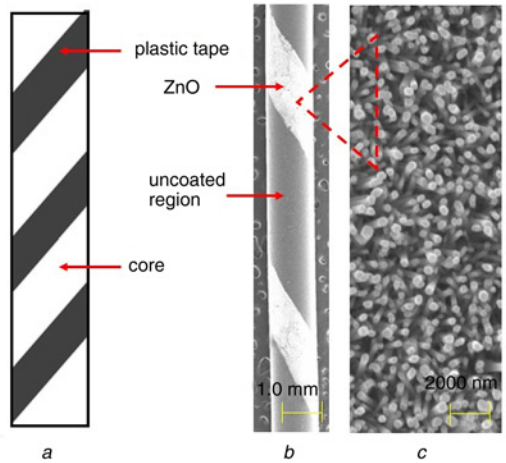

Fig. 3 *Graphical representation and SEM image of*
a Spiral patterned form using plastic tape
b 13 kX SEM image of ZnO spiral patterned growth after synthesis
c 25.0 kX SEM image of the nanorods

doi: 10.1049/mnl.2015.0452

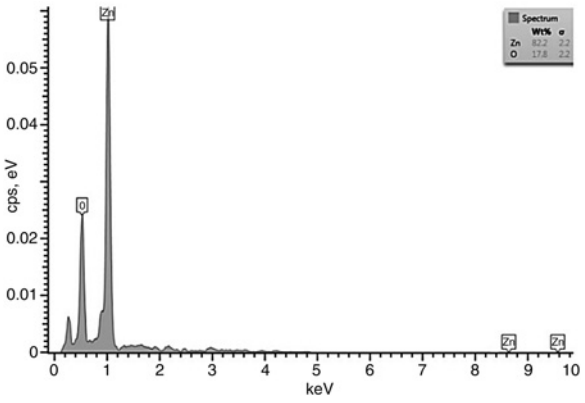

Fig. 4 *EDX spectrum of ZnO nanorods showing zinc and oxygen peaks*

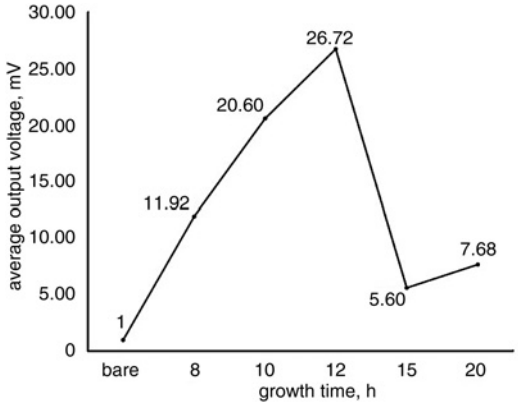

Fig. 6 *Average V_{pp} at interfacial area for all growth times*

evaporate. The process was repeated ten times to ensure optimal seed distribution on the surface of the POF. It was followed by drying the samples at 70 °C under ambient conditions thereby concluding the seeding process.

2.3. ZnO nanorods synthesis: ZnO nanorods were grown following the seeding process. 2.97 g zinc nitrate hexahydrate [$Zn(NO_3)_2{\cdot}6H_2O$] (Ajax Finechem Pty Ltd) and 1.40 g of hexamethyleneteramine or HMT [$(CH_2)_6N_4$] (Sigma-Aldrich) were dissolved in 400 ml of deionised (DI) water to form 10 mM solutions of each compound. The seeded POFs were then vertically placed in 200 ml of the synthesis solution and heated in an oven set at 90 °C. Following 5 h of heating, the solution was discarded and replaced with a new solution in order to maintain constant growth conditions. Growth time was varied from 8 to 20 h. Following synthesis, POFs were removed and rinsed several times in DI water.

2.4. Characterisation: Scanning electron microscopy (SEM) was performed at the National Nanotechnology Center, Thailand Science Park (Hitachi, 3400N). Energy dispersive X-ray (EDX) was performed during SEM. The optical characterisation apparatus is schematically depicted in Fig. 2*a* below. The magnitude of the side coupling was measured in terms of 'peak-to-peak' voltage (V_{pp}) following excitation by a modulated red light source – e.g. the extended light source. Light from the extended source was restricted by an aperture onto specific sites on the POF in order to optimise the growth conditions for maximum side coupling. The egress end of the optical fiber is linked to a digital oscilloscope and subsequently to a computer for data recording and analysis.

2.5. Experimental: V_{pp} was analysed according to the schematic depicted in Fig. 2*a*. POFs were illuminated by a 3 cm diameter broad band light-emitting diode extended light source placed 10 cm from the fiber surface. A rectangular aperture 1 × 3 cm was placed perpendicularly to and directly on top of the fiber during signal acquisition. Three domains were inspected for the unpatterned type of fiber: (i) the interfacial area between the ZnO coating and the uncoated fiber near the detector end; (ii) the middle ZnO domain; and (iii) the tip domain that consisted of the terminal ZnO-air interface. The fiber tip was covered in all cases except for readings taken for the 'tip domain' of the unpatterned and spiral patterned POF. In the figure, dark regions represent

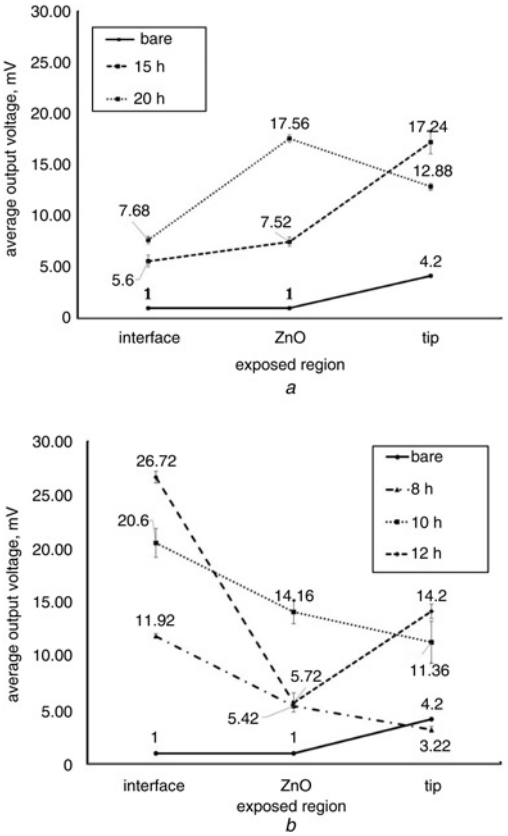

Fig. 5 *Average V_{pp} on bare and unpatterned POFs*
a Average V_{pp} for 15 and 20 h growth time
b Back scattering effect is eliminated at interface regions after reducing the growth time to 8, 10, and 12 h

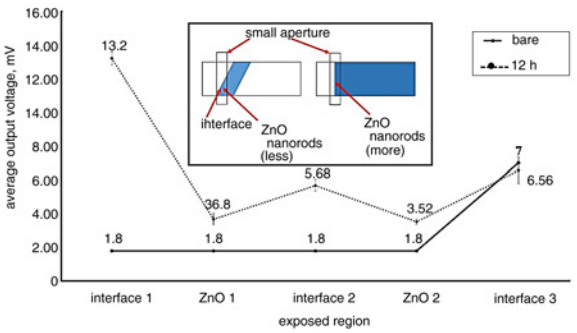

Fig. 7 *Average V_{pp} for the spiral patterned growth for 12 h which has more than one interface and ZnO regions. The inset shows the regions covered by the aperture when characterisation the structured and unstructured ZnO growth on POF*

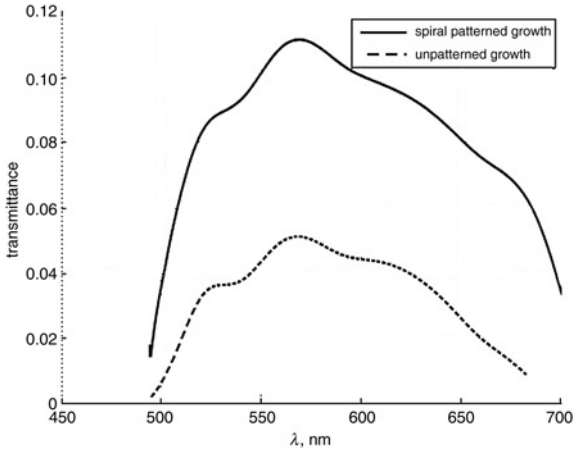

Fig. 8 *Transmittance of the visible white light spectrum*
a Spiral patterned
b Unpatterned growth

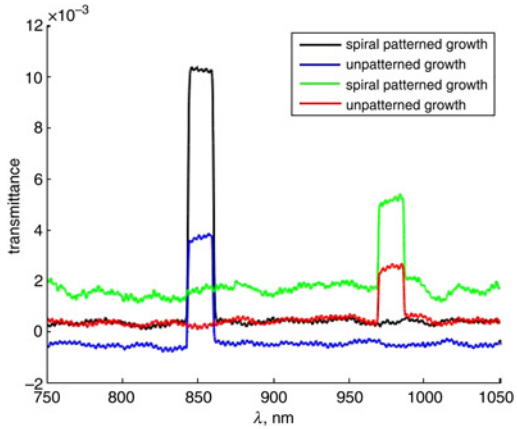

Fig. 9 *Spectrum for near infrared (850 and 980 nm) for spiral patterned and unpatterned growth*

patterned ZnO nanorods scattering domains. For unpatterned POFs, the extended light source was positioned in the centre of the ZnO coated area. V_{pp} was measured on bare and unpatterned ZnO nanorods POFs (variable growth time) to determine side coupling limits. Optimised growth time was applied to V_{pp} measurements on patterned surfaces.

For patterned POFs, five ZnO domains were analysed: (i) the interfacial area between the ZnO coating and the uncoated fiber near the detector end; (ii) the adjacent pure ZnO domain; (iii) a second interfacial domain between the ZnO and the uncoated fiber; (iv) a second pure ZnO domain; and (v) the tip domain of ZnO and air as before (uncovered during tip domain measurements). In all cases, bare POFs devoid of ZnO coating served as controls in the experiments. Five readings were acquired for each measurement.

Spectral analysis was performed for the unpatterned and patterned samples to identify the wavelength coupling maxima using the setup shown in Fig. 2*b*. A broad spectrum white light source and two infrared laser sources were used (850 and 980 nm). The optical transmittance of patterned and unpatterned POFs were compared. No aperture was used during spectral acquisition. Transmittance was calculated by the following expression

$$\text{Transmittance} = \frac{\text{coupled power}}{\text{source power}}$$

3. Result and discussion

3.1. Physical characterisation: SEM image in Fig. 3*b* with magnification set at 13.00 kX was used to observe the ZnO spiral pattern on the POF. Fig. 3*c* depicts SEM images with magnification of 25.00 kX which clearly shows vertical alignment, high density (63 nanorods/1.23×10^{-12} m^2 = 510×10^{11} nanorods/m^2) and uniform distribution of ZnO nanorods on the POF.

EDX elemental analysis revealed that the topcoat layer consisted only of zinc and oxygen as shown in Fig. 4.

3.2. Optical characterisation: The plots in Figs. 5*a* and *b* show the average V_{pp} on bare and unpatterned POFs. Initially the growth duration was set at 15 or 20 h. However, the average V_{pp} at the interface region (for both these growth times) was greatly reduced due to backscattering that limits light side coupling to the core modes (Fig. 5*a*). Longer growth times resulted in higher ZnO nanorods density on POFs and hence, the coating provided a greater barrier to light side coupling due to backscattering. The bare POFs did not show any backscattering effects. The problem was solved by reducing the ZnO nanorods growth duration to 8, 10, or 12 h. Fig. 5*b* shows the improvement in the average V_{pp} for the above mentioned growth durations: 8, 10, and 12 h. From this characterisation, it was determined that the growth duration of 12 h was optimal in limiting backscattering. The conclusion was based on the highest average V_{pp} at the interface region. This optimised process of growing ZnO nanorods on POF was then applied to fabricate the spiral patterned growth as shown in Fig. 3*a*.

The results of optimisation are summarised in Fig. 6 showing only V_{pp} against interface data. At 12 h growth time, V_{pp} is maximised, thereby demonstrating high light side coupling with reduced leakage due to backscattering. Tip readings (uncovered) are high due to ingress of light through the fiber optic in addition to potential side coupling.

The graph of average V_{pp} for the five domains on the spiral patterned growth is depicted in Fig. 7. V_{pp} was highest at Domain 1, the ZnO bare interface closest to the detector. V_{pp} was significantly lower at Domain 2, the pure ZnO region. A slight rise in V_{pp} was observed at Domain 3, another interfacial region. Domain 4, a pure ZnO region located further from the detector showed similar values to Domain 2. Domain 5 showed the tip effect as before. Therefore, the spiral patterned on the POF has potential application as multi-channel excitation and enhance the total coupling inside POF. It is worth mentioning that V_{pp} was a factor of 2× lower than for the same domain on the unpatterned fiber. This is due to area reduction of the spiral structure as shown by the inset in Fig. 7. This is not the case when an extended source was used.

Fig. 8 represents the transmittance of visible white light for spiral patterned and unpatterned POFs when an extended source was used. The result indicates that the spiral patterned growth is able to increase coupling of the light source better than the unpatterned growth due to the existence of more interfacial ZnO regions on the POF. The plot in Fig. 7 also shows that the spiral patterned growth provides a higher light transmittance with an improvement factor of 2.2.

Fig. 9 shows that the transmittance of light for the spiral patterned growth is higher than the unpatterned growth when both infrared laser sources were tested. However, the infrared laser source did not significantly couple at the particular wavelength inside the POF. Therefore, the coupling efficiency was too low for useful applications.

4. Conclusion: The synthesis process to grow ZnO nanorods on POF core is optimised by maximising the side coupling to POF from an extended source. This work also reports a novel spiral patterned growth of ZnO nanorods on POF. The light side coupling improves considerably for spiral patterned growth

doi: 10.1049/mnl.2015.0452

compared with unpatterned growth due to the presence of more ZnO regions on the POF. The spiral pattern on the POF also provides a higher light intensity multi-channel compared with unpatterned ZnO nanorods POF. Spectral analysis is performed to investigate light transmittance for different wavelength of light sources. It is found that visible white light source significantly coupled the light into the POF compared with infrared laser sources. In future, investigation of coupling efficiency can be performed by varying the width and spacing of the coated and uncoated regions.

5. Acknowledgment: The authors would like to acknowledge University of Malaya for financial support under high impact research grant (grant no: D000009-16001).

6 References

[1] Kolodziejczak-Radzimska A., Jesionowski T.: 'Zinc oxide – from synthesis to application: a review', *Materials*, 2014, **7**, (4), pp. 2833–2881

[2] Pauporté T., Lincot D.: 'Electrodeposition of semiconductors for optoelectronic devices: results on zinc oxide', *Electrochim. Acta*, 2000, **45**, (20), pp. 3345–3353

[3] Xiang B., Wang P., Zhang X., *ET AL.*: 'Rational synthesis of p-type zinc oxide nanowire arrays using simple chemical vapor deposition', *Nano Lett.*, 2007, **7**, (2), pp. 323–328

[4] Janotti A., Van de Walle C.G.: 'Fundamentals of zinc oxide as a semiconductor', *Rep. Prog. Phys.*, 2009, **72**, (12), pp. 126501.

[5] Shinde S.S., Shinde P.S., Bhosale C.H., *ET AL.*: 'Optoelectronic properties of sprayed transparent and conducting indium doped zinc oxide thin films', *J. Phys. D, Appl. Phys.*, 2008, **41**, (10), pp. 105109

[6] Chang C.C., Chiu N.F., Lin D.S., *ET AL.*: 'High-sensitivity detection of carbohydrate antigen 15-3 using a gold/zinc oxide thin film surface plasmon resonance-based biosensor', *Anal. Chem.*, 2010, **82**, (4), pp. 1207–1212

[7] Kumar S.A., Chen S.M.: 'Nanostructured zinc oxide particles in chemically modified electrodes for biosensor applications', *Anal. Lett.*, 2008, **41**, (2), pp. 141–158

[8] Kong T., Chen Y., Ye Y., *ET AL.*: 'An amperometric glucose biosensor based on the immobilization of glucose oxidase on the ZnO nanotubes', *Sens. Actuators B, Chem.*, 2009, **138**, (1), pp. 344350

[9] Cao H., Zhao Y.G., Ong H.C., *ET AL.*: 'Ultraviolet lasing in resonators formed by scattering in semiconductor polycrystalline films', *Appl. Phys. Lett.*, 1998, **73**, (25), pp. 3656–3658

[10] Rasmussen J.W., Martinez E., Louka P., *ET AL.*: 'Zinc oxide nanoparticles for selective destruction of tumor cells and potential for drug delivery applications', *Expert Opin. Drug Deliv.*, 2010, **7**, (9), pp. 10631077

[11] Lenz A.G., Karg E., Lentner B., *ET AL.*: 'A dose-controlled system for air-liquid interface cell exposure and application to zinc oxide nanoparticles', *Part. FibreToxicol.*, 2009, **6**, (32), pp. B16

[12] Johnson J.C., Yan H., Schaller R.D., *ET AL.*: 'Near-field imaging of nonlinear optical mixing in single zinc oxide nanowires', *Nano Lett.*, 2002, **2**, (4), pp. 279–283

[13] Zvyagin A.V., Zhao X., Gierden A., *ET AL.*: 'Imaging of zinc oxide nanoparticle penetration in human skin in vitro and in vivo', *J. Biomed. Opt.*, 2008, **13**, (6), 064031-9

[14] Fallah H., Harun S.W., Mohammed W.S., *ET AL.*: 'Excitation of core modes through side coupling to multimode optical fiber by hydrothermal growth of ZnO nanorods for wide angle optical reception', *J. Opt. Soc. Am. B*, 2014, **31**, (9), pp. p2232-2238

[15] Batumalay M., Harith Z., Rafaie H.A., *ET AL.*: 'Tapered plastic optical fiber coated with ZnO nanostructures for the measurement of uric acid concentrations and changes in relative humidity', *Sens. Actuators A, Phys.*, 2014, **210**, pp. 190–196

[16] Lokman A., Harun S.W., Harith Z., *ET AL.*: 'Inline Mach–Zehnder interferometer with ZnO nanowires coating for the measurement of uric acid concentrations', *Sens. Actuators A. Phys.*, 2015, **234**, pp. 206–211

[17] Harith Z., Irawati N., Rafaie H.A., *ET AL.*: 'Tapered plastic optical fiber coated with Al-doped ZnO nanostructures for detecting relative humidity', *IEEE Sens. J.*, 2015, **15**, (2), pp. 845–849

[18] Chen J.J., Zeng F., Li D.M., *ET AL.*: 'Deposition of high-quality zinc oxide thin films on diamond substrates for high-frequency surface acoustic wave filter applications', *Thin Solid Films*, 2005, **485**, (1), pp. 257–261

[19] Bora T., Fallah H., Chaudhari M., *ET AL.*: 'Controlled side coupling of light to cladding mode of ZnO nanorods coated optical fibers and its implications for chemical vapor sensing', *Sens. Actuators B, Chem.*, 2014, **202**, pp. 543–550

[20] Fallah H., Chaudhari M., Bora T., *ET AL.*: 'Demonstration of side coupling to cladding modes through zinc oxide nano-rods grown on multimode optical fiber', *Opt. Lett.*, 2013, **38**, (18), pp. 3620–3622